

# Z-scan technique for saturable absorption using diffraction method in $\gamma$ -alumina nanoparticles

E. Koushki · M. H. Majles Ara · H. Akherat Doost

Received: 2 January 2013 / Accepted: 25 July 2013 / Published online: 4 August 2013  
© Springer-Verlag Berlin Heidelberg 2013

**Abstract** In this article, the  $z$ -scan method has been corrected for the case of saturation in absorption. Using the principle relations of the changes in the transmitted beam through a Kerr sample and Fresnel–Kirchoff integral method, a proper model is offered to evaluate the electric field in any point of the far field. This model contains both the saturation intensity and nonlinear refractive index simultaneously. Based on this study, a precise method to evaluate the nonlinear indices is obtained. Finally, this model is used in the precise study of  $z$ -scan curves for  $\gamma$ -Al<sub>2</sub>O<sub>3</sub> nanocolloid and its saturation intensity and nonlinear refractive index have been obtained precisely.

## 1 Introduction

In 1989, Sheik-bahae et al. [1] introduced  $z$ -scan method to obtain nonlinear optical coefficients of materials using a single laser beam and enveloped it in 1990 [2]. In this method, first, a thin sample containing only nonlinear refractive index was considered and then the phase shift of the electric field of the transmitted beam was studied in the far field by using the Gaussian decomposition method [3, 4]. Nonlinear refractive index could be a result of electron

transition nonlinearity, reorientation effect or thermal lensing nonlinearity, or a mixture of them [5, 6]. In the next step, they represented a more complete phase shift of the electric field containing both the nonlinear refractive and absorption indices [2], but the electric field was preceded till the outer surface of the sample and was not evaluated in the far field. Also, the nonlinear absorption index was only due to two photon absorption mechanisms that could be used for saturated absorption regime only in intensities lower than the saturation intensity ( $I_s$ ). This technique was developed for more general cases as Hermite–Gaussian beams [7] and elliptic Gaussian beams [8]. Gu et al. [9] have presented a theoretical investigation on the open-aperture Gaussian beam  $z$ -scan technique for dominant saturable absorption cases, by using the Adomian decomposition (AD) method, and their worked was developed for close-aperture  $z$ -scan technique using AD method [10]. In the next papers [11, 12], Fresnel–Kirchoff integral method was used to relate the far-field electric field to the transmitted beam through the sample. This method could be used for any kind of the beam phase shifts and does not confine choosing the phase shift [12]. In [13], a more complete model was offered that the electric field in far field was related to the output beam from the surface of the sample and the phase shift containing both the refraction and absorption nonlinearities. This model used the basic relations of the two photon absorptions (TPA) presented in Sheik-bahae et al. [2]. In this work, we introduce a proper model for the cases that the mechanism of saturation in absorption (SA) is responsible for nonlinear absorption. We propose new relations to evaluate saturation intensity and refractive index, and using Fresnel–Kirchoff integral, we obtain a complete model for the electric field of the transmitted beam containing both the nonlinear indices and uses no approximations.

E. Koushki (✉) · M. H. Majles Ara · H. Akherat Doost  
Photonics Laboratory, Physics Department, Kharazmi  
University, Tehran, Iran  
e-mail: ehsan.koushki@yahoo.com

E. Koushki  
Physics Department, Hakim Sabzevari University,  
Sabzevar, Iran

### 2 Theory

SA could be defined as [14]:

$$\alpha(I) = \frac{\alpha_0}{1 + I/I_s} \tag{1}$$

where  $\alpha_0 = N\sigma_1$ ,  $I$  and  $I_s$  are the unsaturated (linear) absorption, input intensity and the saturation intensity, respectively.  $N$  and  $\sigma_1$  are the number of absorbers per unit volume and the single-photon absorption cross-section, respectively. Taylor expansion of this relation gives the following:

$$\begin{aligned} \alpha(I) &= \alpha_0 \left( 1 + \sum_{n=1}^{\infty} (-1)^n \left(\frac{I}{I_s}\right)^n \times \binom{n}{n!} \right) \\ &= \alpha_0 - \frac{\alpha_0}{I_s} I + \frac{\alpha_0}{I_s^2} I^2 - \dots \end{aligned} \tag{2}$$

In TPA regime, we have [15];

$$\alpha(I) = N\sigma_1 + N\sigma_2 I = \alpha_0 + \beta I \tag{3}$$

where  $\sigma_1$  is the TPA cross-section.

It is obvious that in the case  $I/I_s \ll 1$ , Eq. 2 turns to Eq. 3 with  $\beta = -\alpha_0/I_s$ , so it is permissible to use open- and close-aperture  $z$ -scan relations of [2]. But as  $I$  increases in comparison with  $I_s$ , more precise relations are required.

Assuming a TEM<sub>00</sub> Gaussian beam of beam waist radius  $w_0$  traveling in the  $+z$  direction, we could write the electric field as [2, 4]:

$$\begin{aligned} E(z, r) &= E_0 \frac{w_0}{w(z)} \exp \left\{ -i \left( kz - \tan^{-1} \left( \frac{z}{z_0} \right) \right) \right\} \\ &\quad \exp \left\{ -r^2 \left( \frac{1}{w^2(z)} + \frac{ik}{2R(z)} \right) \right\}, \end{aligned} \tag{4}$$

where  $E_0$ ,  $w(z) = w_0 \sqrt{1 + \frac{z^2}{z_0^2}}$ ,  $z_0 = kw_0^2/2$  and  $R(z) = z(1 + z_0^2/z^2)$  are the electric field at beam waist of the Gaussian beam, the beam radius at  $z$ , the diffraction length of the beam and the radius of curvature of the wavefront at  $z$ , respectively. The beam waist (focal point) is located at  $z = 0$ . The light intensity of the beam could be obtained by

$$I(z, r) = \frac{nc\epsilon_0}{2} |E(z, r)|^2 = I_0 \left( \frac{1}{1 + \left(\frac{z}{z_0}\right)^2} \right) \exp \left( -\frac{2r^2}{w^2(z)} \right), \tag{5}$$

where  $I_0 = \frac{nc\epsilon_0}{2} |E_0|^2$ . The equations describing the propagation of the optical field inside the nonlinear material take the following form:

$$\frac{d\Delta\varphi}{dz'} = -\Delta n(I)k \tag{6}$$

and

$$\frac{dI}{dz'} = -\alpha(I)I. \tag{7}$$

Consider that a Gaussian beam passes through a thin third-order nonlinear optical sample with nonlinear refraction  $n_2$  located at  $z$  [1, 2]. In the case of a cubic nonlinearity and negligible nonlinear absorption, Eq. 6 can be solved to give the on-axis nonlinear phase shift at the center of the beam focus as

$$\Delta\varphi_0 = -kn_2 I_0 L_{\text{eff}} = -k\Delta n L_{\text{eff}}, \tag{8}$$

and correspondingly, the radial and position ( $z$ ) variations of the phase shift at the exit surface of the sample would be

$$\Delta\varphi(z, r) = \frac{\Delta\varphi_0}{1 + \left(\frac{z}{z_0}\right)^2} \exp(-2r^2/w^2(z)). \tag{9}$$

where  $z$ ,  $L_{\text{eff}} = (1 - e^{-\alpha_0 L})/\alpha_0$ ,  $L (< z_0)$  and  $\Delta n = n_2 I_0$  are the distance between the sample and the beam waist, the effective length of the sample, the sample thickness and the refraction change, respectively. In [12, 13], the electric field at the exit plane of the sample has been obtained and the electric field in the far field has been evaluated by means of free-space Fresnel-Kirchhoff diffraction integral at the Fraunhofer approximation. Based on this formulation, close-aperture  $z$ -scan curves have been obtained. The above-mentioned formulation is proper in the cases where the nonlinear absorption is considered small or the effect of nonlinear absorption is removed from the close-aperture  $z$ -scan curve (e.g., by dividing the close-aperture curve to the open one).

In the presence of nonlinear absorption, the transmitted beam contains both the nonlinear absorption and refraction effects. In the case of TPA nonlinearity, a proper modeling has been performed previously [13]. Here, we focus only on the SA.

Returning to Eqs. 1 and 7, one could write the intensity distribution on the exit plane of the sample:

$$I_e(z, r) = I(z, r) e^{-\alpha(z,r)L} = I(z, r) \exp \left( -\frac{\alpha_0}{1 + \frac{I(z,r)}{I_s}} L \right), \tag{10}$$

and for the electric field:

$$E_e(z, r) = E(z, r) \exp \left( -\frac{\alpha_0}{2 \left( 1 + \frac{I(z,r)}{I_s} \right)} L \right) \exp(i\Delta\varphi(z, r)). \tag{11}$$

We could obtain the modified nonlinear phase shift containing nonlinear absorption and refractions. Equations 1, 6 and 7 give the following:

$$\frac{d\Delta\varphi}{dz'} = -kn_2 \left( -\frac{1}{\alpha_0} \right) \left( 1 + \frac{I}{I_s} \right) \frac{dI}{dz'}; \tag{12}$$

thus, the nonlinear phase shift at the exit surface of the sample would be

$$\Delta\varphi(z, r) = -kn_2 \left( L_{\text{eff}} I(z, r) + L_{\text{eff}}^{(2)} \frac{I^2(z, r)}{I_s} \right) \tag{13}$$

where  $L_{\text{eff}}^{(2)} = \frac{1 - \exp(-2\alpha_0 L)}{2\alpha_0}$ . Also, the nonlinear phase shift at the center of beam focus would be (Eq. 9)

$$\Delta\varphi_0 = -kn_2 \left( L_{\text{eff}} I_0 + L_{\text{eff}}^{(2)} \frac{I_0^2}{I_s} \right). \tag{14}$$

Now, we could write the electric field on the exit surface of the sample as

$$E_e(r, z) = E_0 \frac{w_0}{w(z)} \exp(-i(kz - \text{Arc tan}(z/z_0))) \times \exp\left( \frac{-ikr^2}{2R(z)} - \frac{r^2}{w^2(z)} + i\Delta\varphi(z, r) - \frac{1}{2}\alpha(z, r)L \right). \tag{15}$$

The electric field in the far field is obtained by means of free-space Fresnel–Kirchhoff diffraction integral at the Fraunhofer approximation. For a radial symmetric field, it equals a Hankell of Fourier–Bessel transform of the field, namely

$$E(\rho, z) = \frac{1}{i\lambda D} \int_0^\infty J_0(k\theta r) E_e(r, z) 2\pi r dr, \tag{16}$$

where  $J_0(x)$ ,  $\theta$  and  $\rho$  are the zero-order Bessel function of the first kind, the far-field diffraction angle and the radial coordinate in the far-field observation plane, respectively. In the paraxial approximation, distance from the exit plane of the medium to the far-field observation plane ( $D$ ) is related to the radial coordinate and the diffraction angle by  $\rho = D\theta$ . Therefore, we can write:

$$E(\rho, z) = \left( \frac{2\pi}{i\lambda D} \right) \times E_0 \frac{w_0}{w(z)} \exp(-i(kz - \arctan(z/z_0))) \times \int_0^\infty J_0\left(\frac{k\rho r}{D}\right) \exp\left\{ -\frac{ikr^2}{2R(z)} - \frac{r^2}{w^2(z)} - ikn_2 \left( L_{\text{eff}} I(z, r) + L_{\text{eff}}^{(2)} \frac{I^2(z, r)}{I_s} \right) - \frac{\alpha_0}{2 \left( 1 + \frac{I(z, r)}{I_s} \right)} \right\} r dr. \tag{17}$$

Also, we can write the distribution pattern of irradiance as:

$$I(\rho, z) = I' \left| \int_0^\infty J_0\left(\frac{k\rho r}{D}\right) \times \exp\left( -\frac{ikr^2}{2R(z)} - \frac{r^2}{w^2} + i\Delta\varphi(z, r) - \frac{\alpha(z, r)}{2} \right) r dr \right|^2, \tag{18}$$

where

$$I' = \frac{cn_0\epsilon_0}{2} \times \left( \frac{1}{\lambda D} \right)^2 \times (2\pi E_0)^2 \left( \frac{w_0}{w(z)} \right)^2. \tag{19}$$

The magnitude of  $E_0$  can be calculated simply through  $\frac{2}{w_0} \sqrt{\frac{P_0}{c\epsilon_0 n_0 \pi}}$ , where  $P_0$  is the laser output power.

Equations 17–19 describe perfectly the electric field and the intensity irradiation of the transmitting beam through a Kerr sample with SA in the far field. Furthermore, it is suitable for cases with high optical nonlinearity that may include diffraction ring patterns [12]. The main virtue of these relations is that the effect of all linear and nonlinear optical coefficients of the sample is presented in one formulation simultaneously.

Open-aperture z-scan curves could properly been described using Eq. 10. Transmitted power in open-aperture curve is

$$P(z) = \int_{r=0}^\infty I_e(z, r) 2\pi r dr \tag{20}$$

That could be normalized to unity. In close-aperture setup, a finite aperture of linear transmittance  $S = 1 - \exp\left(-\frac{2r_a^2}{w_a^2}\right)$  ( $r_a$  and  $w_a$  being the aperture radius and the beam radius at the aperture plane, respectively) has been assumed, which is placed at the far field so that the aperture center is located at the beam center. The normalized transmitted power through the aperture can be simply calculated by:

$$T_{\text{norm}}(z) = \frac{\int_{\rho=0}^{r_a} I(\rho, z, n_2, I_s) 2\pi \rho d\rho}{\int_{\rho=0}^{r_a} I(\rho, z, n_2 = 0, I_s = \infty) 2\pi \rho d\rho} \tag{21}$$

This formulation for close-aperture curve includes both the saturation intensity and refraction effects.

### 3 Experimental results and discussion

Here, we study third-order nonlinear optical properties of  $\gamma\text{-Al}_2\text{O}_3$  nanospheres [16] using the above formulations.  $\gamma$ -alumina nanocrystallites were prepared by the in-flight thermal plasma method and then a plasma reactor was used

for the production of this powder. In this process, 99.9 % of pure aluminum powder with an average size of  $\sim 40 \mu\text{m}$  got vaporized and reacted completely with oxygen, and finally, these nanoparticles were synthesized [16]. The sample was observed by FETEM (Fig. 1) that shows the range of 7–56 nm in the nanoparticle size with mean diameter of about 22 nm (Fig. 2).

X-ray diffraction has been used to identify the crystal structure (phase). Figure 3 illustrates the XRD pattern of samples prepared under optimized processing condition. The diffraction pattern showed several broad but prominent peaks that are mostly attributed to  $\gamma$ -phase  $\text{Al}_2\text{O}_3$ . The sample also showed some peaks of  $\delta$ -alumina, but no aluminum or any other phase of aluminum oxide, such as  $\alpha$ - $\text{Al}_2\text{O}_3$ , or other compound, such as aluminum nitride, was observed. That is because the aluminum nitride requires nitrogen atmosphere and higher temperature ( $>1,800 \text{ }^\circ\text{C}$ ) to form.

A colloidal solution containing about  $0.5 \text{ g l}^{-1}$  of nanoparticles in water was poured into a 1-mm-thick quartz cell and utilized in these experiments.

Using SA model, we reevaluate the nonlinear optical indices and estimate the precise of usual model (TPA model) in such cases.

In experimental setups, a 50-mW He–Ne laser beam with wavelength of 633 nm was focused on a waist of  $w_0 = 42 \mu\text{m}$  and produced the intensity of  $I_0 = 1,805 \text{ W cm}^{-2}$  in this point.

A colloid of the nanospheres in ethanol is prepared. The linear absorption in this wavelength is  $18.5 \text{ cm}^{-1}$ . Experimental open-aperture  $z$ -scan curve is plotted in Fig. 4. Using the TPA model [2],

$$P(z) = P_0 e^{-zL} \frac{\ln[1 + q_0(z)]}{q_0(z)} \quad \text{and} \quad (22)$$

$$q_0(z) = \beta I_0 L_{\text{eff}} / (1 + z^2/z_0^2)$$

The numerical curve (solid curve in Fig. 4) and correspondingly the nonlinear absorption coefficient are

obtained  $\beta = -2.53 \times 10^{-3}$ . Using the first-order approximation of Eq. 2, one could obtain  $I_s = -\alpha_0/\beta = 7,321 \text{ W cm}^{-2}$ . But using Eq. 10 and the least square fitting (the residual sum of squares [13]), we

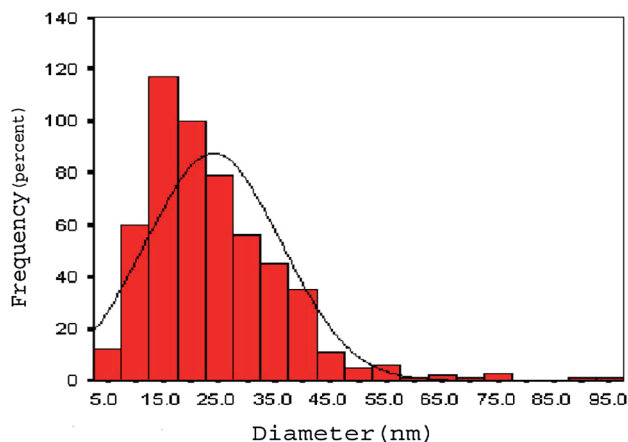


Fig. 2 Histogram of FETEM images of  $\gamma$ - $\text{Al}_2\text{O}_3$  nanocrystallites

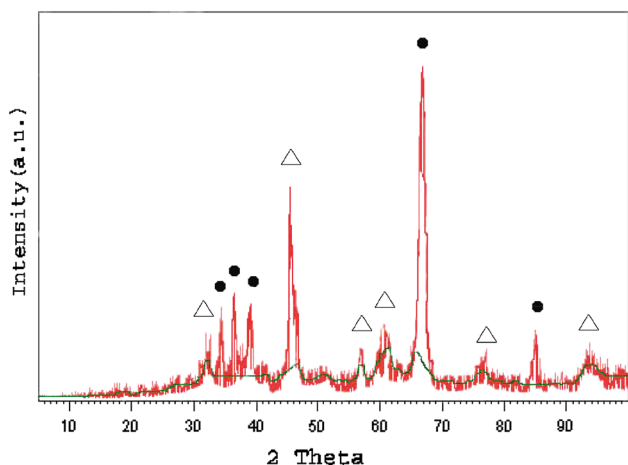
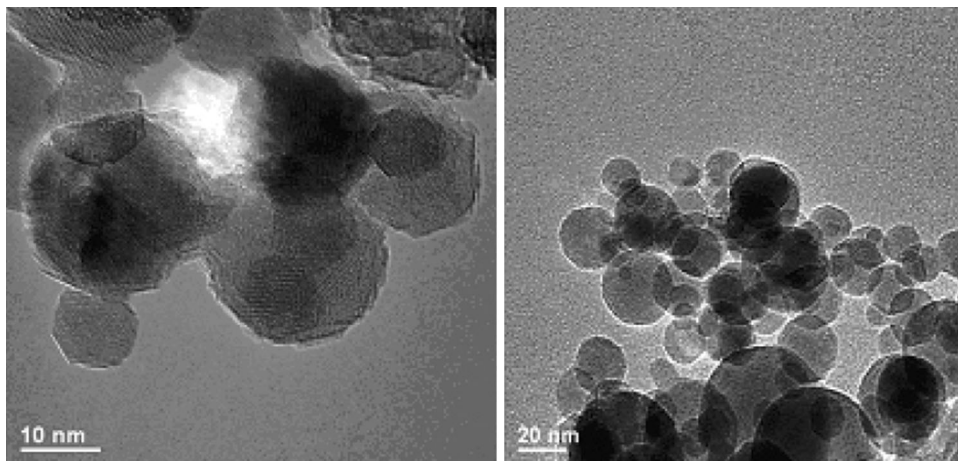
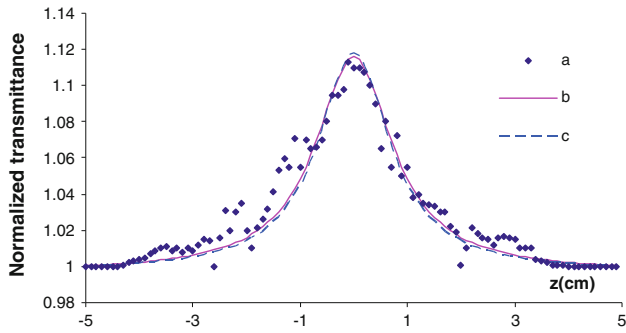


Fig. 3 XRD pattern of  $\gamma$ - $\text{Al}_2\text{O}_3$  nanocrystallites. Filled circle  $\gamma$ -alumina. Open triangle  $\delta$ -alumina

Fig. 1 FETEM image of  $\gamma$ - $\text{Al}_2\text{O}_3$  nanocrystallites





**Fig. 4** *a* Experimental open-aperture data. *b* Numerical fitted curve using Eq. 22 (TPA Model). *c* Numerical fitted curve using Eq. 20 (SA model)

found that with  $I_s = 13,850 \text{ W cm}^{-2}$ , the best fitted curve to the experimental data could be obtained (dashed curve in Fig. 3). This shows that the contribution of other terms in Eq. 2 could not be considered negligible and also using TPA model is not accurate.

The next step is finding the nonlinear refractive index. A finite aperture of linear transmittance  $S = 0.09$  has been utilized. Substituting the measured value of  $I_s$  in Eq. 21 and using the least square fitting, the best value for the nonlinear refractive index is obtained  $n_2 = -4.68 \times 10^{-8} \text{ cm}^2 \text{ W}^{-1}$  (Fig. 5).

Now, this new model is checked through comparison with the pure close-aperture curve, which is the simplest model and contains only nonlinear refraction [2, 13]. In this model, the electric field at the exit surface of the sample is

$$E_e(r, z) = E_0 \frac{w_0}{w(z)} \exp(-i(kz - \text{Arc tan}(z/z_0))) \times \exp\left(\frac{-ikr^2}{2R(z)} - \frac{r^2}{w^2(z)} + i\Delta\varphi(z, r) - \alpha_0 L/2\right), \tag{23}$$

where  $\Delta\varphi(z, r)$  is determined using Eqs. 8 and 9, and the electric field in far field could be obtained using Eq. 16. This model does not contain nonlinear absorption and could be used for both the TPA and SA mechanisms. In

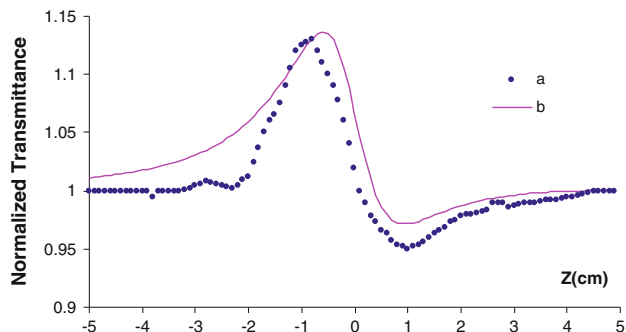


**Fig. 5** *a* Experimental close-aperture data. *b* Numerical fitted curve using Eqs. 17 and 21 (SA model)

Fig. 5, substituting  $n_2 = -4.68 \times 10^{-8} \text{ cm}^2 \text{ W}^{-1}$  in Eq. 22, the pure close-aperture curve has been obtained.

In TPA model, the division of the close-aperture curve (containing both the nonlinear absorptive and refractive nonlinearities) to the open aperture one gave pure close-aperture curve (only contains nonlinear refractive index). SA model should satisfy similar conditions. In Fig. 6, the close-aperture curve obtained from Eq. 21 has been divided to open aperture one and pure close-aperture curve is obtained. This curve is in good agreement with the resulted curve from Eq. 23. This could fairly back up new SA model.

Figure 7 shows the output power versus input one using the above-mentioned laser that its maximum power is 50 mW. The maximum intensity reached by this laser is  $I_0 = 1,805 \text{ W cm}^{-2}$  at the center of the focal point. Earlier, the saturation intensity was obtained,  $I_s = 13,850 \text{ W cm}^{-2}$ , which is very higher than  $I_0$ . Therefore, the saturation intensity is not detectable from the output–input intensity (power) curve using the above-mentioned laser (Fig. 7). But using the open-aperture curve and Eqs. 10 and 20, the saturation intensity has been obtained using this low-power laser. In Fig. 7, the sample was put at the focus and theoretical output power has been reached by integrating  $I_e(r, z = 0)$  (Eq. 10) over the exit surface of the sample:

$$P_e(z = 0) = \int_{r=0}^{\infty} 2\pi r I(z = 0, r) \exp\left(-\frac{\alpha_0}{1 + \frac{I(z=0,r)}{I_s}} L\right) dr. \tag{24}$$

The optical nonlinearity of aqua samples applied with continued wave laser beam is usually contributed to two additional mechanisms: thermo-optical (thermal) effect and reorientation Kerr effect in liquids [6]. Experiments show that the nonlinearity due to electron transition (such as saturable absorption and TPA) has some contribution to the nonlinear refraction but have main effect on nonlinear

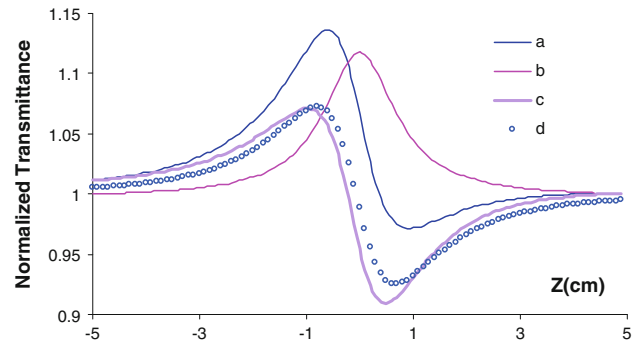


**Fig. 6** *a* Theoretical real close-aperture curve using Eqs. 17, 18 and 21 (SA model). *b* Theoretical open-aperture curve using Eq. 20 (SA model). *c* Pure close-aperture curve obtained by dividing curves *a*–*b*. *d* Pure close-aperture curve using Eqs. 8, 9 and 23



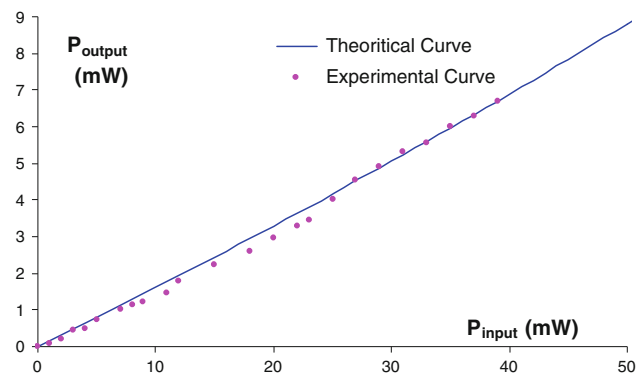


**Fig. 7** Output power versus input one as the sample located at  $z = 0$

absorption, in CW regime. Reorientation Kerr effect occurs in molecules or particles with different polarizabilities along their principle axes so is negligible in spherical nanoparticles. It is non-resonant and therefore associated with the real part of susceptibility [6]. Thermal lensing effect is an inevitable process in CW laser illuminations and prevails in other processes in nonlinear refraction, here.

#### 4 Conclusion

In summary,  $z$ -scan formulations have been specialized for the cases with SA using Fresnel–Kirchhoff integral method. These formulations obtain a perfect description of the light electric field in the far field that is useful to interpret the open- and close-aperture  $z$ -scan results, far-field intensity distributions, diffraction rings and so on. This method was examined for  $z$ -scan results of  $\gamma$ -alumina nanocolloids and gave new values for optical nonlinear coefficients.

#### References

1. M. Sheik-bahae, A.A. Said, E.W. Van Stryland, High-sensitivity, single-beam  $n_2$  measurements. *Opt. Lett.* **14**, 955–957 (1989)

2. M. Sheik-bahae, A.A. Said, T.H. Wei, D.J. Hagan, E.W. Van Stryland, Sensitive measurement of optical nonlinearity using a single beam. *IEEE J. Quantum Electron.* **26**, 760–769 (1990)
3. D. Weaire, B.S. Wherrett, D.A.B. Miller, S.D. Smith, Effect of low-power nonlinear refraction on laser beam propagation in InSb. *Opt. Lett.* **4**, 331–333 (1974)
4. G. Tsigaridas, M. Fakis, I. Polyzos, P. Persephonis, V. Giannetas, Z-scan analysis for high order nonlinearities through Gaussian decomposition. *Opt. Commun.* **225**, 253–268 (2003)
5. L. Palfalvi, J. Hebling, Z-scan study of the thermo-optical effect. *Appl. Phys. B* **78**, 775–780 (2004)
6. R.W. Boyd, *Nonlinear Optics*, 3rd edn. (Academic Press, New York, 2007)
7. G. Tsigaridas, M. Fakis, I. Polyzos, M. Tsibouri, P. Persephonis, V. Giannetas, Z-scan analysis for near-Gaussian beams through Hermite–Gaussian decomposition. *J. Opt. Soc. Am. B* **20**, 670–676 (2003)
8. G. Tsigaridas, M. Fakis, I. Polyzos, P. Persephonis, V. Giannetas, Z-scan technique for elliptic Gaussian beams. *Appl. Phys. B* **77**, 71–75 (2003)
9. B. Gu, Y.X. Fan, J. Wang et al., Characterization of saturable absorbers using an open-aperture Gaussian-beam Z scan. *Phys. Rev. A*, **73** (2006) Article ID 065803
10. X. Liu, Y. Tomita, Closed-aperture Z-Scan analysis for nonlinear media with saturable absorption and simultaneous third- and fifth-order nonlinear refraction. *Phys. Res. Int.* **2012** (2012), Article ID 161572, 9 pp
11. J. Wang, M. Sheik-Bahae, A.A. Said, D.J. Hagan, E.W. Van Stryland, Time-resolved Z-scan measurements of optical nonlinearities. *J. Opt. Soc. Am. B* **11**, 1009–1017 (1994)
12. E. Koushki, A. Farzaneh, S.H. Mousavi, Closed aperture  $z$ -scan technique using the Fresnel–Kirchhoff diffraction theory for materials with high nonlinear refractions. *Appl. Phys. B* **99**, 565–570 (2010)
13. M.H. Majles Ara, E. Koushki, Data analysis of  $z$ -scan experiment using Fresnel–Kirchhoff integral method in colloidal  $\text{TiO}_2$  nanoparticles. *Appl. Phys. B* **107**, 429–434 (2012)
14. W. Demtröder, *Laser Spectroscopy*, vol. 1 and 2, 4th edn. (Springer, Berlin, 2008)
15. R. Schroeder, B. Ullrich, Absorption and subsequent emission saturation of two-photon excited materials: theory and experiment. *Opt. Lett.* **27**, 1285–1287 (2002)
16. P. Boroojerdian, M.H. Majles Ara, Z. Javadi, B. Akbari, T. Karimi, Synthesis and nonlinear optical characterization of nanocrystalline  $\gamma$ -alumina produced by in-flight thermal plasma route. *Eur. Phys. J. Appl. Phys.* **53**, 30401 (2011)